compared to that over the Arabian Sea. The greater dominance of finer aerosol particles during the summer season is observed over the coastal regions of the Bay of Bengal compared to those over the Arabian Sea, which indicates greater influence of the continental aerosols over the Bay of Bengal. The particle size distribution during the winter season over the Bay of Bengal and the Arabian Sea is found to be unimodal, whereas during the summer season, it is characterized by bimodal distribution. Higher concentration of the larger particles over the coastal regions of the Arabian Sea during summer is due to the dry conditions prevailing in the western part of the Indian subcontinent and larger transport of dust particles from the continent. An interesting low-AOD zone has been found over the Bay of Bengal.

1. Jaenicke, R., *Aerosols and their Climatic Effects* (eds Gerbard, H. E. and Deepak, A.), Deepak Publishers, USA, 1984, pp. 7–34.
2. Parameswaran, K., *Proc. Indian Natl. Sci. Acad.*, 1998, **64**, 245–266.
3. Charlson, R. J., Lovelock, J. E., Andrea, M. O. and Warren, S. G., *Nature*, 1987, **326**, 655–661.
4. Hoppel, W. A., Fitzgerald, J. W., Frick, G. M. and Larson, R. E., *J. Geophys. Res.*, 1990, **95**, 3659–3686.
5. Rao, Y. Jaya and Devara, P. C. S., *Curr. Sci.*, 2001, **80**, 120–122.
6. Murugavel, P., Pawar, S. D. and Kamra, A. K., *ibid*, 2001, **80**, 123–127.
7. Moorthy, K. K., Saha, Auromeet and Niranjan, K., *ibid*, 2001, **80**, 145–150.
8. Ramanathan, V. *et al.*, Indian Ocean Experiment, White Paper, C[4], Scripps Institution of Oceanography, La Jolla, CA 92093–0221, USA, 1995.
9. Niranjan, K. *et al.*, *Tellus*, 1997, **49B**, 439–446.
10. Doerffer, R. GKSS 92/E/54, GKSS-Forschungszentrum Geesthacht GMBH, 1992.
11. Indian Remote Sensing Satellite IRS P4 (OCEANSAT) Handbook, National Remote Sensing Agency, Department of Space, Government of India, Hyderabad, 1999.
12. Gordon, H. R., *J. Geophys. Res.*, 1997, **102**, 17081–17106.
13. Okada, Y., Mukai, S. and Sano, I., *J. Indian Soc. Remote Sensing*, 2002 (in press).
14. Rajeev, K., Ramanathan, V. and Meywerk, J., *J. Geophys. Res.*, 2000, **105**, 2029–2043.
15. Angstrom, A., *Tellus*, 1961, **13**, 214–223.
16. Shaw, G. E., Regan, J. A. and Herman, B. M., *J. Appl. Meteorol.*, 1973, **12**, 374–380.
17. Satheesh, S. K., *Curr. Sci.*, 2002, **82**, 310–316.
18. Moorthy, K. Krishna, Nair, Prabha R. and Murthy, B. V. Krishna, *J. Appl. Meteorol.*, 1990, **30**, 844–852.
19. Moorthy, K. Krishna, Pillai, Preetha S., Saha, Auromeet and Niranjan, K., *Curr. Sci.*, 1999, **76**, 961–967.
20. Moorthy, K. Krishna, Satheesh, S. K. and Murthy, B. V. Krishna, *J. Atmos. Solar-Terr. Phys.*, 1998, **60**, 981–992.

ACKNOWLEDGEMENTS. The OCM data were available to R.P.S. through the ISRO-AO project. The work was supported by a grant under ISRO-GBP programme from the Indian Space Research Organization, Bangalore to R.P.S. We thank the anonymous reviewers for their comments and suggestions.

Received 9 April 2002; revised accepted 19 September 2002

New chemical shift signatures of bound calcium in EF-hand proteins

H. S. Atreya and K. V. R. Chary*

Department of Chemical Sciences, Tata Institute of Fundamental Research, Mumbai 400 005, India

We present two new chemical shift signatures for monitoring the state of bound calcium (Ca^{2+}) in NMR studies of EF-hand proteins. They have been observed in the form of large upfield chemical shifts (1–1.5 ppm) for (i) $H^{\beta 1}/H^{\beta 2}$ and (ii) $^{13}C^{\beta}$ resonances of a conserved Asp residue at the first position of 12 amino acid residue long Ca^{2+}-binding loops, going from Ca^{2+}-free (apo) to the Ca^{2+}-bound (holo) form of protein. In the apo form, both the $H^{\beta 1}/H^{\beta 2}$ and $^{13}C^{\beta}$ spins are found to resonate at their normal chemical shift values. Such upfield-shifted resonances of the Asp residue, in the holo-form, are shown to arise due to the ring current effect of a conserved Phe/Tyr residue at –4 position, preceding the same Ca^{2+}-binding loop. This is illustrated in the case of calmodulin and four other proteins, belonging to the family of EF-hand proteins.

EF-hand proteins belong to a growing family of calcium (Ca^{2+})-binding proteins, with more than 1000 distinct sequences known and catalogued into 66 different subfamilies[1]. These proteins, which function as signal transducers or modulators, have been a subject of great interest for structural biologists, resulting in the availability of three-dimensional (3D) structures for more than 100 of them as of today[2]. The most well-studied proteins in this family are calmodulin (CaM)[3], troponin C (TnC)[4], calbindin[5] and parvalbumin[6].

The canonical Ca^{2+}-binding motif in EF-hand proteins consists of a contiguous 12-residue loop flanked by two helices forming the so-called 'EF-hand motif'[7]. According to the convention, such Ca^{2+}-binding sequence is termed the EF-'loop' or the Ca^{2+}-binding loop, although the last three positions in it initiate the second helix (or the F-helix). Each of the flanking helices is amphiphilic and possesses four conserved hydrophobic residues at positions –1, –4, –5 and –8 in the first helix (E-helix), and positions 13, 16, 17 and 20 in the second helix (F-helix)[7]. The numbering is relative to the Ca^{2+}-binding loop. In such canonical Ca^{2+}-binding loop, the specific sites labelled as *X*, *Y*, *Z*, *–Y*, *–X*, *–Z* in Table 1, refer to 1st, 3rd, 5th, 7th, 9th and 12th positions respectively, in the Ca^{2+}-binding loops of the protein, which co-ordinate to Ca^{2+} in a pentagonal bi-pyramidal geometry[7]. Out of these, residues at positions 1, 3, 5 and 12 co-ordinate directly to Ca^{2+} via their side-chain carboxylate/carbonyl groups. Table 1 shows the primary sequence of Ca^{2+}-

*For correspondence. (e-mail: chary@mailhost.tifr.res.in)

Table 1. Primary sequences of EF-hand Ca^{2+}-binding loops from five different proteins. Ca^{2+}-binding sites have been numbered beginning with an invariant Asp residue at position 1 and ending at the 12th position with an invariant Glu residue. Phe residues at –4 position in the Ca^{2+}-binding loops have been highlighted for clarity

Protein	Ca^{2+}-binding loop*	–4		*X* 1	2	*Y* 3	4	*Z* 5	6	*–Y* 7	8	*–X* 9	10		*–Z* 12
*Eh*CaBP#	I	**F**6	• • •	**D**	V	N	G	D	G	A	V	S	Y	E	E21
	II	**F**42	• • •	**D**	A	D	G	N	G	E	I	D	Q	N	E57
	III	Y81	• • •	**D**	V	D	G	D	G	K	L	T	K	E	E96
	IV	V113	• • •	**D**	A	N	G	D	G	Y	I	T	L	E	E128
Calmodulin	I	**F**16	• • •	**D**	K	D	G	D	G	T	I	T	T	K	E31
	II	I52	• • •	**D**	A	D	G	N	G	T	I	D	F	P	E67
	III	**F**89	• • •	**D**	K	D	G	N	G	Y	I	S	A	A	E104
	IV	I125	• • •	**D**	I	D	G	D	G	Q	V	N	Y	E	E140
Troponin C	I	**F**26	• • •	**D**	A	D	G	G	G	D	I	S	T	K	E41
	II	I62	• • •	**D**	E	D	G	S	G	T	I	D	F	E	E77
	III	**F**102	• • •	**D**	K	N	A	D	G	F	I	D	I	E	E117
	IV	M138	• • •	**D**	K	N	N	D	G	R	I	D	F	D	E153
Calbindin	II	**F**51	• • •	**D**	K	N	G	D	G	E	V	S	F	E	E66
Parvalbumin	II	**F**47	• • •	**D**	A	D	A	S	G	F	I	E	E	E	E62
	III	**L**86	• • •	**D**	K	D	G	D	G	L	I	G	I	D	E101

*Within the Ca^{2+}-binding loop, residues that are involved in co-ordination with Ca^{2+} in a pentagonal bi-pyramidal geometry are 1, 3, 5, 7, 9 and 12 (which are labelled as sites *X*, *Y*, *X*, *–Y*, *–X* and *–Z* respectively).
#Ca^{2+}-binding protein from *Entamoeba histolytica*.

binding loops from five different EF-hand proteins that have been chosen in the present study. The most conserved amino acid residue in the Ca^{2+}-binding loops of EF-hand proteins is the Asp residue at position 1 (hereafter referred to as D1)[8] (see Table 1). Both the oxygen (OD1 and OD2) atoms belonging to the side-chain carboxylate group of D1 are involved in extensive hydrogen bonding interactions with other residues in the respective Ca^{2+}-binding loops and hence, the protein does not tolerate even a small structural perturbation that would disturb such interactions. Substitution of D1 with other amino acid residues has been shown to result in 10–100-fold loss in the Ca^{2+}-binding affinity[8]. Another amino acid residue, which has also been found to be highly conserved across EF-hand proteins, is a Phe residue, which is part of the E-helix and at position –4 (hereafter referred to as F(-4)), prior to the Ca^{2+}-binding loop (Table 1). In a study involving 567 EF-hand sequences, it was found that 50% of the sequences have F(-4) in the vicinity of respective Ca^{2+}-binding loops[8].

The presence of an invariant D1 and a highly conserved F(-4) in EF-hand proteins suggests that these residues can be used as probes to monitor structural changes in this class of Ca^{2+}-binding proteins. During the course of our NMR study[9] involving a Ca^{2+}-binding protein from *Entamoeba histolytica* (*Eh*CaBP), we found that in the Ca^{2+}-bound (holo) state, one of the $H^{\beta1}/H^{\beta2}$ and $^{13}C^{\beta}$ spins of D1 exhibits upfield shifts as large as 1.0–1.2 ppm (refs 9 and 10) with respect to the random coil values[11]. Subsequently, analysis carried out in four other EF-hand proteins revealed that similar upfield shifts of $H^{\beta1}/H^{\beta2}$ and $^{13}C^{\beta}$ spins belonging to D1 occur, in the holo-state, in all Ca^{2+}-binding loops that have a F(-4) in their vicinity, and not otherwise. A statistical analysis of a total of 8381 D ($H^{\beta1}/H^{\beta2}$) and 2176 D ($^{13}C^{\beta}$) chemical shifts from 1846 entries in the BioMagResBank (BMRB)[12], reveals that only 0.90% of the total D($H^{\beta1}/H^{\beta2}$) spins and 12% of the total D($^{13}C^{\beta}$) spins resonate below 1.80 and 39.0 ppm respectively. The plots for these analysis are shown in Figure 1. Further, most of these upfield-shifted resonances belong to D1 ($H^{\beta1}/H^{\beta2}$ and $^{13}C^{\beta}$) spins in EF-hand proteins. Interestingly, in the Ca^{2+}-free (apo) state of the protein, both $H^{\beta1}/H^{\beta2}$ and $^{13}C^{\beta}$ spins of D1 have the usual chemical shift values.

In this communication we explain the structural origin of such unusual upfield shifts of $H^{\beta1}/H^{\beta2}$ and $^{13}C^{\beta}$ spins of D1, in holo EF-hand proteins. In NMR studies, such chemical shift signatures serve as evidences for confirming whether the protein is in a Ca^{2+}-bound state or not. In the past, two other signatures for probing the state of bound Ca^{2+} in EF-hand proteins have been proposed. They correspond to the downfield shift of the amide proton of a conserved Gly at position 6 (ref. 13) and ^{15}N resonance of the amino acid residue at position 8 in the Ca^{2+}-binding loop[14], upon binding of Ca^{2+} to the protein.

Chemical shifts and 3D structures of proteins used in the present analyses were obtained from BMRB and Protein Data Bank (PDB) respectively. The BMRB accession numbers are the following: *Eh*CaBP (Holo: 4271); Troponin C (Holo: 4080); Calbindin (Holo: 247, Apo: 327); Parvalbumin (Holo: 144). The PDB codes are the following: *Eh*CaBP (Holo: 1JFK); Calmodulin (Holo:

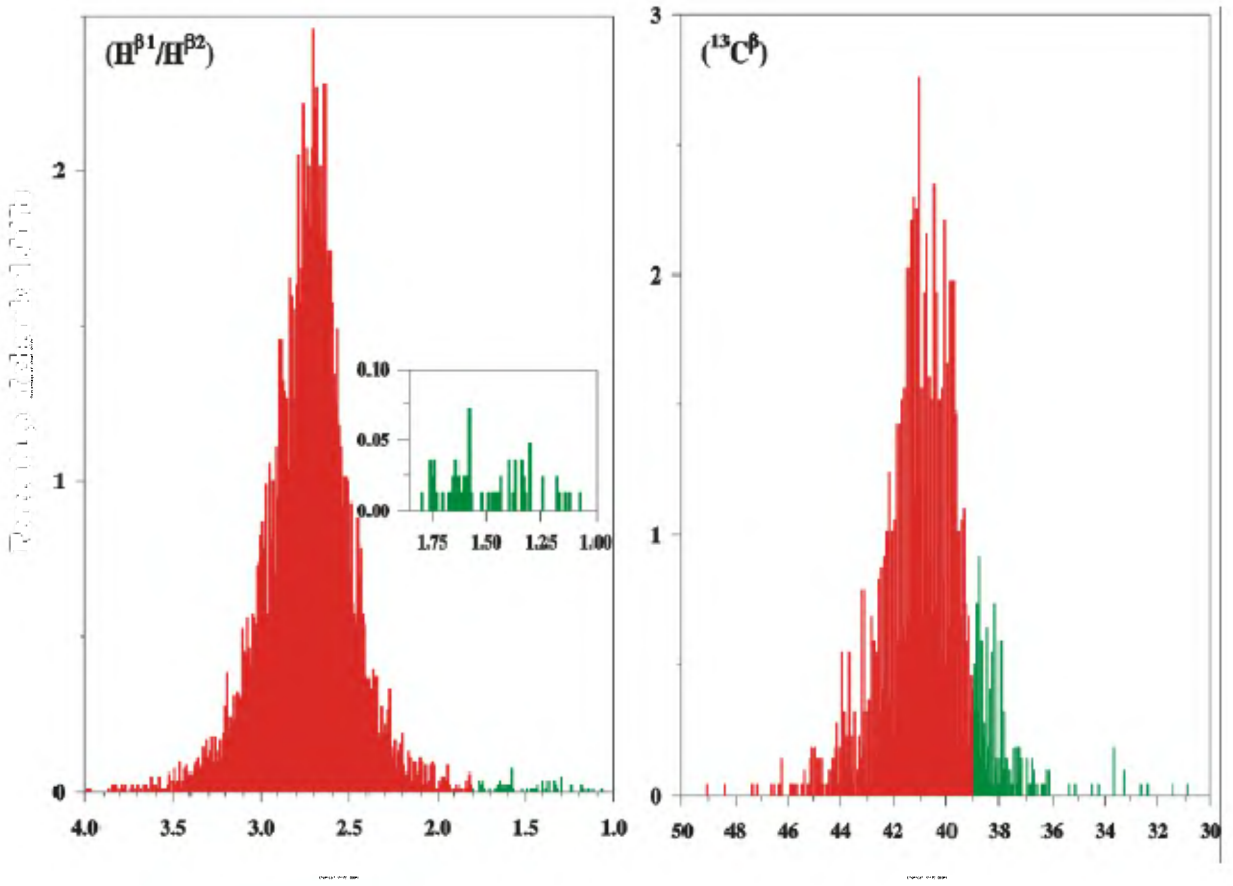

Figure 1. Distribution of Asp $H^{\beta1}/H^{\beta2}$ and $^{13}C^{\beta}$ chemical shifts in proteins. Histograms depict the percentage of chemical shifts that lie within a range of 0.01 to 0.02 ppm for ^{1}H and ^{13}C chemical shifts respectively. Histograms for Asp $H^{\beta1}/H^{\beta2}$ and $^{13}C^{\beta}$ spins that resonate below 1.80 and 39 ppm respectively, are shown in green. Histograms for Asp $H^{\beta1}/H^{\beta2}$ that resonate below 1.80 ppm have been expanded and shown in red as well as an inset for clarity.

Table 2. Experimentally observed $H^{\beta1}/H^{\beta2}$ and $^{13}C^{\beta}$ chemical shifts of D1 containing a F(-4) in the respective Ca^{2+}-binding loops in both apo and/or holo states of five proteins

		$H^{\beta1}/H^{\beta2}$						$^{13}C^{\beta}$ δ(ppm)	
		Holo			Apo				
Protein	D1	δ(ppm)	Θ(in deg)[a]	*r* (in Å)[a]	δ(ppm)	Θ(in deg)[a]	*r* (in Å)[a]	Holo	Apo
*Eh*CaBP	D10	**1.60**/2.52	8.1/21.0	4.9/5.3	*	*		39.0	*
	D46	**2.20**/2.68	40.5/56.6	3.8/5.1	*	*		38.7	*
	D85	**1.80**/2.87	35.0/62.6	4.1/4.6	*	*		38.5	*
Calmodulin	D20	**1.57**/2.44	34.9/46.6	3.5/4.3	**2.35**/2.84	58.0/60.0	4.8/6.5	38.9	39.8
	D93	**1.45**/2.38	26.3/36.6	3.8/4.4	**2.56**/3.18	79.0/86.0	7.7/8.1	38.3	39.5
Troponin C	D30	**1.46**/2.56	27.5/38.1	4.2/5.6	*	*		38.9	*
	D106	**1.47**/2.47	16.3/23.0	5.8/6.9	*	*		39.1	*
Calbindin	D54	**1.60**/2.52	20.5/21.30	3.2/4.1	**2.53**/2.71	33/36.87	3.5/4.2	*	*
Parvalbumin	D51	**1.45**/2.44	47.4/57.0	4.1/5.4	*	*		*	*

*, Not available.
[a]Angle Θ and distance *r*, according to Scheme 1 are shown for each $H^{\beta1}/H^{\beta2}$ atom of D1.

1CLL (X-ray), Apo: 1CFD (NMR)); Troponin C (Holo: 1TNX (NMR)); Calbindin (Holo: 2BCB (NMR), Apo: 1CLB (NMR)) and Paravalbumin (Holo: 3PAT (X-ray)). Chemical shifts of apo and holo CaM were obtained from the laboratories of M. Ikura and Ad Bax respectively (pers. commun.). In none of the proteins, stereospecific

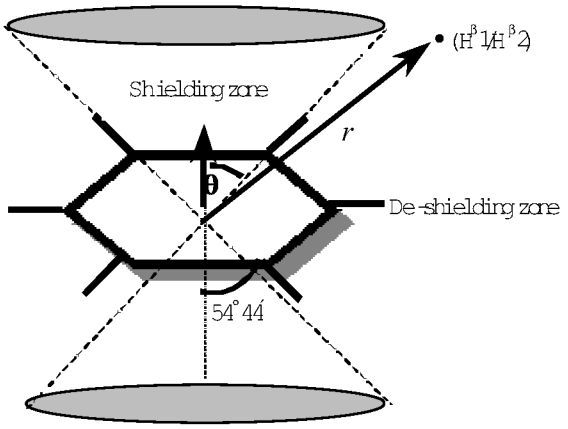

Scheme 1.

NMR assignments of $H^{\beta 1}$ and $H^{\beta 2}$ spins were available and hence, both H^{β} spins are referred to as $H^{\beta 1}/H^{\beta 2}$ throughout the communication. All the structural models presented here were generated using MOLMOL[15].

The ring current effect due to F(-4)/Y(-4), on the H^{β} and $^{13}C^{\beta}$ resonances of D1 has been analysed using the popular Haigh–Mallion model[16]. The contribution of the ring current effect to secondary shifts of both H^{β} and $^{13}C^{\beta}$ spins, i.e. the difference between the observed resonance and its random-coil chemical shift, has been obtained using MOLMOL. Such a contribution is computed as a sum of magnetic anisotropy effect due to the pi-electron cloud in the aromatic ring and electrostatic polarization of the C–H bonds.

Experimentally observed $H^{\beta 1}/H^{\beta 2}$ and $^{13}C^{\beta}$ chemical shifts for individual D1 residues present in five proteins chosen for the present study, are shown in Table 2. Chemical shifts of only those D1 residues that have F(-4)/Y(-4) with respect to the same Ca^{2+}-binding loop are shown (the corresponding primary sequence of the loops is shown in Table 1). The D1 that lacks F(-4)/Y(-4) does not exhibit the upfield shifts and hence, is not discussed here. The average chemical shift of the upfield-

Table 3. The contribution of ring current to the secondary shift of D1 ($H^{\beta 1}/H^{\beta 2}$ and $^{13}C^{\beta}$) resonances. The total secondary shifts (δ_c) for each D1 ($H^{\beta 1}/H^{\beta 2}$ and $^{13}C^{\beta}$) spin has been partitioned into ring current (RC) contribution and contribution due to other effects. A random coil value of 2.75 and 39.8 ppm has been used for calculating the secondary shifts for Asp H^{β} and $^{13}C^{\beta}$ spins, respectively

		$H^{\beta 1}/H^{\beta 2}$					
		Holo δ_c (ppm)		Apo δ_c (ppm)		δ_c (Holo) – δ_c (Apo) (ppm)	
Protein	D1	RC	Other	RC	Other	RC	Other
*Eh*CaBP	D10	–0.98/–0.58	–0.17/0.35	*		*	
	D46	–0.72/–0.83	0.17/0.76	*		*	
	D85	–0.50/–0.01	–0.45/0.13	*		*	
Calmodulin	D20	–1.10/–0.18	–0.08/–0.13	–0.21/–0.25	–0.19/0.34	–0.90/0.07	0.11/–0.47
	D93	–1.38/–0.71	0.08/0.34	0.02/0.13	–0.21/0.3	–1.40/–0.84	0.29/0.04
Troponin C	D30	–1.17/–0.68	–0.12/0.39	*		*	
	D106	–1.50/–0.60	0.22/0.32	*		*	
Calbindin	D54	–1.27/–0.90	0.12/0.67	–0.99/–0.51	0.74/0.47	–0.28/–0.37	–0.62/0.20
Parvalbumin	D51	–0.60/–0.25	–0.70/–0.06	*		*	
		$^{13}C^{\beta}$					
		Holo δ_c (ppm)		Apo δ_c (ppm)		δ_c (Holo) – δ_c (Apo) (ppm)	
Protein	D1	RC	Other	RC	Other	RC	Other
*Eh*CaBP	D10	–0.81	0.01	*		*	
	D46	–0.13	–1.10	*		*	
	D85	–0.30	–1.00	*		*	
Calmodulin	D20	–0.27	–0.63	–0.73	0.73	0.46	–1.36
	D93	–1.40	–0.10	–0.24	–0.06	–1.16	–0.04
Troponin C	D30	–0.79	–0.11	*		*	
	D106	–1.00	0.30	*		*	

*, Not available.

shifted H^{β} and $^{13}C^{\beta}$ resonances are found to be 1.60 ± 0.24 and 38.7 ± 0.28 ppm respectively. On the other hand, in the apo-state of the protein, chemical shifts of the same H^{β} and $^{13}C^{\beta}$ spins are within the standard values of 2.70 ± 0.29 and 40.70 ± 1.70 ppm respectively.

In order to have an insight about the influence of F(-4)/Y(-4) on the $H^{\beta 1}/H^{\beta 2}$ spins of D1 residue, the ring current effects were measured in terms of the angle Θ, made by the line joining $H^{\beta 1}/H^{\beta 2}$ and the centre of F(-4)/Y(-4) ring with the normal to the plane of the ring, and the distance r, as shown in Scheme 1. The angles Θ and the distances r derived from the PDB structures are listed in Table 2 for individual $H^{\beta 1}/H^{\beta 2}$ spins.

Table 3 shows the net contribution of the ring current effect to the secondary shifts of $H^{\beta 1}/H^{\beta 2}$ and $^{13}C^{\beta}$ spins of D1 in holo and/or apo state, along with its contribution to the difference in the chemical shifts between the apo and holo states of five proteins, used in the present study. The total secondary shift for each D1 in Table 3 has been partitioned into ring current contribution and contribution due to other effects (such as magnetic anisotropy of the CN, CO bond and electrostatic effects). As is evident from Table 3, on the whole, the ring current effect due to F(-4)/Y(-4), in the holo form, contributes to an extent of 80% and above to the total secondary shift of the upfield-shifted D1 $H^{\beta 1}/H^{\beta 2}$ and $^{13}C^{\beta}$ spins. This is also evident from the angle Θ (see Table 2), which indicates that the upfield-shifted $H^{\beta 1}/H^{\beta 2}$ of D1 in the holo protein lies in the shielding cone. On the other hand, in the apo-state, for both $H^{\beta 1}/H^{\beta 2}$ and $^{13}C^{\beta}$ spins, the angle Θ and the distance r from the centre of the ring increase (see Table 2). This leads to a fall in the ring current effect, resulting in the de-shielding and concomitant downfield shift of the respective resonances. Although both the $H^{\beta 1}/H^{\beta 2}$ spins experience a downfield shift in their resonances from holo- to apo-state, it is more pronounced for one of the

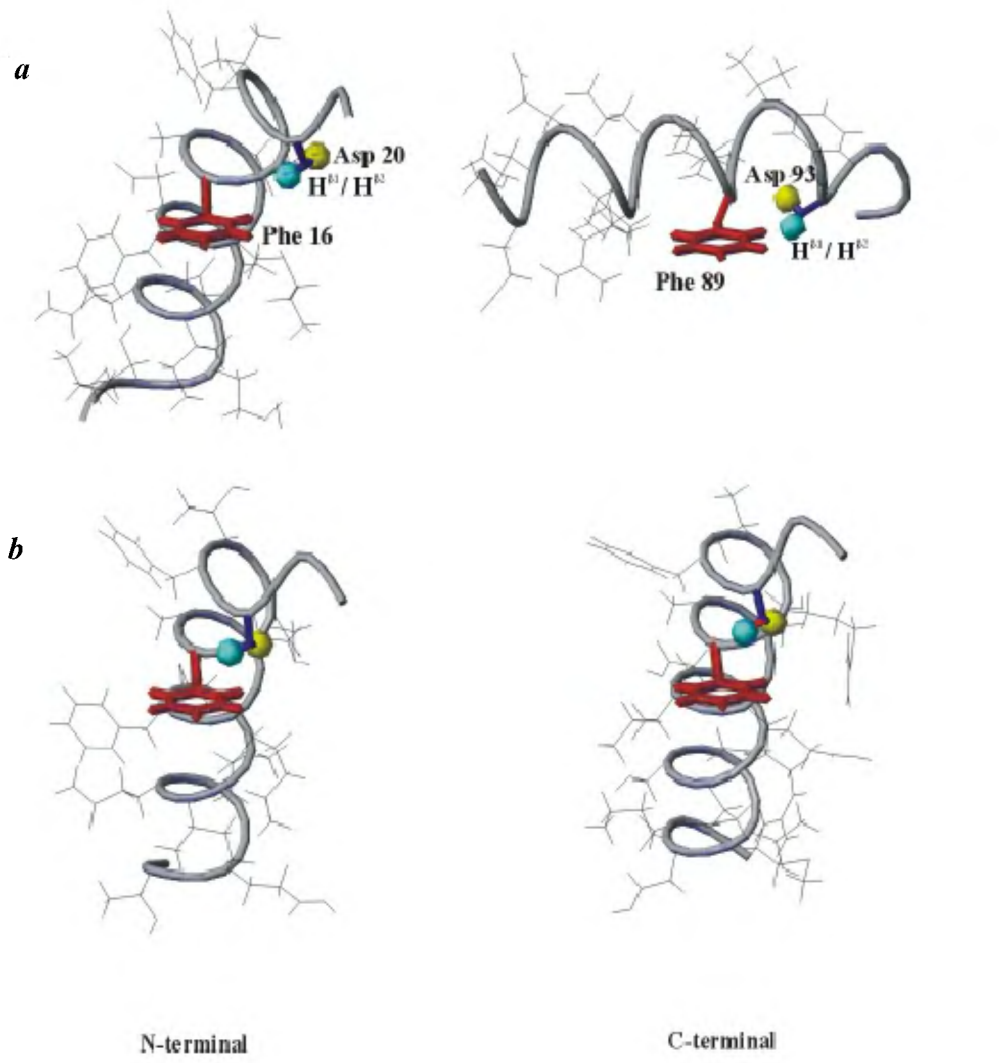

Figure 2. Structural transition from (***a***) apo to (***b***) holo form for Ca^{2+}-binding loops I (in N-terminal domain) and III (in C-terminal domain) of CaM. The F(-4) ring in each loop is shown in red and the D1 ($H^{\beta 1}/H^{\beta 2}$) spin which shows an unusual upfield shift is shown in blue and its geminal partner in yellow.

$H^{\beta1}/H^{\beta2}$ spins (see Table 3), which lies closer to the ring normal (evidenced from the respective lower values of θ and r) compared to its geminal partner. The discrepancy between the observed and calculated chemical shifts (see Table 3) for the $^{13}C^{\beta}$ spin of D46 and D85 in *Eh*CaBP and that of D20 in CaM can be attributed to the error resulting from the approximations used in theoretical ring current calculations.

Marked structural changes as indicated in Table 2, between the holo- and apo-states of EF-hand proteins, are illustrated in Figure 2 *a* and *b* in the case of CaM. CaM possesses two globular domains (N- and C-terminal), each containing a pair of EF-hands[3]. The EF-hand, Ca^{2+}-binding loops I and III in each of these domains contain the conserved F(-4) (Table 1). Figure 2 *a* and *b* corresponds to the apo- and holo-states of CaM respectively. As discussed above, in the apo-state of the protein, the $H^{\beta1}/H^{\beta2}$ are away from the aromatic ring of F(-4) and lie in the de-shielding zone, with their $H^{\beta1}/H^{\beta2}$ resonances downfield-shifted. In the holo-state, these atoms move closer to the centre of the ring and thereby enter the shielding zone. In this state, one of the $H^{\beta1}/H^{\beta2}$ spins is closer to the centre of the ring (shown in blue colour in Figure 2) compared to its geminal partner (shown in yellow), resulting in a dramatic upfield shift of the former. Further, the movement of $H^{\beta1}/H^{\beta2}$ atoms close to the centre of the ring also results in an upfield shift of the $^{13}C^{\beta}$ spin compared to its chemical shift in the apo-state (Table 2).

In conclusion, observation of large upfield shifts of $H^{\beta1}/H^{\beta2}$ spins of D1 can be taken as a signature for verifying whether Ca^{2+} is bound to a given Ca^{2+}-binding loop in EF-hand proteins. This raises the question as to how easy is it to track and assign such unusual chemical shifts? It is indeed easy and straightforward. For example, either a homonuclear (^1H–^1H) 2D TOCSY or a 2D NOESY experiment of the protein recorded in 100% ^2H_2O can distinctly reveal such large upfield shifts of $H^{\beta1}/H^{\beta2}$ spins of an Asp residue involved in coordination with a Ca^{2+}. As mentioned above, earlier signatures were based on the downfield shift of the amide proton of a conserved Gly at position 6 (ref. 13) and ^{15}N resonance of the amino acid residue at position 8 in the Ca^{2+}-binding loop[14], upon binding of Ca^{2+} to the protein. Both these residues do not coordinate with Ca^{2+}. Hence, observation of the large upfield shifts of $H^{\beta1}/H^{\beta2}$ spins of D1 not only reveals the holo state of the Ca^{2+}-binding proteins, but it can also form a right justification for incorporating explicit Ca^{2+}-ligand distances in the refinement stage of NMR-derived structures of holo EF-hand proteins[10]. Further, upfield shifts in $^{13}C^{\beta}$ resonance of D1 as observed here, have implications in 3D structural studies of EF-hand proteins by NMR. First, the upfield shift of D1 $^{13}C^{\beta}$ due to the ring current effect should be taken into account when evaluating its chemical shift index (CSI)[17], since it will otherwise be erroneously classified as belonging to an α-helix instead of the beginning of a loop. Secondly, the large upfield shifts for the $^{13}C^{\beta}$ spin of D1, should be taken into account when chemical shifts are used as constraints in 3D structure calculations. It has been observed earlier that such upfield shift in $^{13}C^{\beta}$ spins can introduce an angle error as high as 40° in structure calculations due to the sensitive nature of the ϕ ψ surfaces[18].

1. Kawasaki, H., Nakayama, S. and Kretsinger, R. H., *BioMetals*, 1998, **11**, 277–295.
2. Nelson, M. R. and Chazin, W. J., *ibid*, 1998, **11**, 297–318.
3. Babu, Y. S., Sack, J. S., Greenhough, T. J., Bugg, C. E., Means, A. R. and Cook, W. J., *Nature*, 1985, **315**, 37–40.
4. Slupsky, C. M. and Sykes, B. D., *Biochemistry*, 1995, **34**, 15953–15964.
5. Akke, M., Drakenberg, T. and Chazin, W., *ibid*, 1992, **31**, 1011–1020.
6. Kretsinger, R. H. and Nockolds, *J. Biol. Chem.*, 1973, **248**, 3313–3326.
7. Falke, J. J., Drake, S. K., Hazard, A. L. and Peersen, O. B., *Q. Rev. Biophys.*, 1994, **27**, 219–290.
8. Linse, S. and Forsén, S., *Adv. Sec. Mesg. Phospho Res.*, 1995, **30**, 89–151.
9. Sahu, S. C., Atreya, H. S., Chauhan, S., Bhattacharya, A., Chary, K. V. R. and Govil, G., *J. Biomol. NMR*, 1999, **14**, 93–94.
10. Atreya, H. S., Sahu, S. C., Bhattacharya, A., Chary, K. V. R. and Govil, G., *Biochemistry*, 2001, **48**, 14392–14403.
11. Bundi, A. and Wüthrich, K., *Biopolymers*, 1979, **18**, 285–297.
12. Seavey, B. R., Farr, E. A., Westler, W. M. and Markley, J. M., *J. Biomol. NMR*, 1991, **1**, 217–236.
13. Akerfeldt, K. S., Coyne, A. N., Wilk, R. R., Thulin, E. and Linse, S., *Biochemistry*, 1996, **35**, 3662–3669.
14. Bieofsky, R. R., Martin, S. R., Browne, J. P., Bayle, P. M. and Feeney, J., *ibid*, 1998, **37**, 7617–7629.
15. Koradi, R., Billeter, M. and Wüthrich, K., *J. Mol. Graph*, 1996, **14**, 51–55.
16. Haigh, C. W. and Mallion, R. B., *Prog. NMR Spectrosc.*, 1980, **13**, 303–344.
17. Wishart, D. S. and Sykes, B. D., *J. Biomol. NMR*, 1994, **4**, 174–180.
18. Iwadate, M., Asakura, T. and Williamson, M. P., *ibid*, 1999, **13**, 199–211.

ACKNOWLEDGEMENTS. Facilities provided by the National Facility for High Field NMR, supported by Department of Science and Technology, Department of Biotechnology, Council of Scientific and Industrial Research, and Tata Institute of Fundamental Research, Mumbai are gratefully acknowledged.

Received 27 May 2002; revised accepted 16 October 2002